Multiscale Surface Field Verification for Ensemble Tropical Cyclone Forecasts

D. Smith, M. Naughton and A. Sulaiman

The Centre for Australian Weather and Climate Research

Introduction

Ensemble forecasts are expected to play an important future role in extreme weather events, such as tropical cyclones, which inflict damage and destruction in Northern Australia during southern hemisphere summers. Tropical cyclone forecasting remains deficient for both track and intensity, which can be partially addressed by ensembles. In this study, regional ensemble forecasts of some recent tropical cyclones in the Australian region are verified against analyses in a multiscale framework, with a focus on mean sea level pressure (MSLP), and 10 metre winds.

The AGREPS Regional Forecast

ACCESS is the Australian Community Climate Earth Simulation System [5], and AGREPS is its global and regional ensemble prediction system, analogous to the UK MET OFFICE MOGREPS [1]. A 24 member global ensemble, with horizontal resolution 90km and 50 vertical levels, drives its regional counterpart on a domain extending from -65°S to 17.125° N, 65°E to 184.6°E, with 0.375° (40km) resolution. Regional short range forecasts extend to 72 hours, convenient for tropical cyclone lifespans.

Multiscale Verification

Multiscale verification applies standard verification procedures to filtered forecast results and analyses, representing selected spatial scales. Planetary, synoptic and subsynoptic scales were considered by Jung and Leutbecher [3], by wavenumber domain partitioning on the ECMWF global ensemble. Four spatial scales, along meridional segments, were provided by an orthonormal wavelet transform for multiscale regional forecast verification in [7].

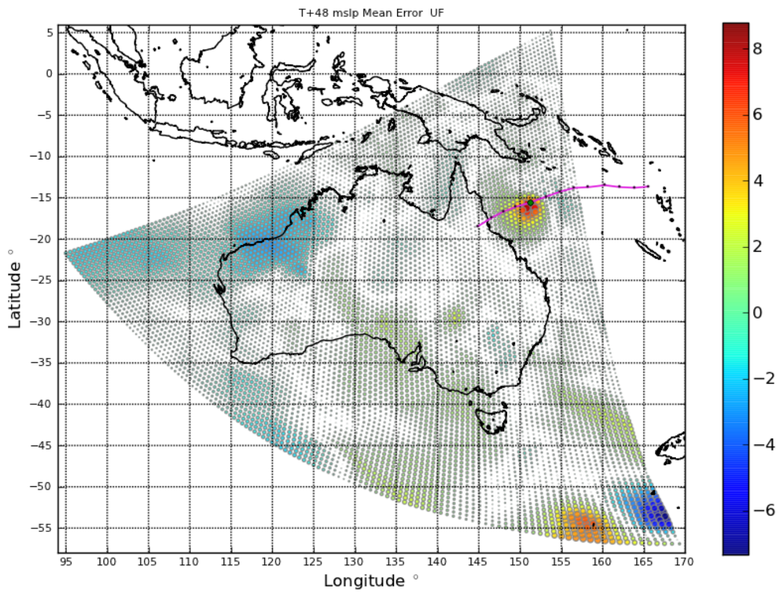

Figure 1: Quasi uniform geodesic grid, comprising 8385 points, constructed by 7 subdivisions of a spherical equilateral (icosahedral) triangle covering the Australian continent. Grid values shown are the mean MSLP error (ensemble mean-analysis) at T+48 for the TC YASI forecast. Also included is the analysis track estimate, which enters the triangular subdomain between T+24 and T+30.

To facilitate a multiscale error-spread analysis, this study employs a modified spherical wavelet transform of the type introduced by Schröder and Sweldens [6], implemented by the Lifting Scheme on a spherical triangular subdomain positioned over the Australian continent, shown in Figure 1. This triangular subdomain is identical to one of 20 spherical equilateral triangles that constitute an icosahedron, and is subdivided 7 times, producing a quasi-uniform geodesic grid hierarchy [4, 2]. Prior to verification calculations, forecast and analysis data is interpolated from the parent latitude-longitude grid onto the new triangular sub-domain [8].

Wavelets by the Lifting Scheme

For wavelet construction, the Lifting Scheme [6] is eminently capable of handling curved surfaces, bounded domains, and irregular sampling, all of which are present in the mesh hierarchy of Figure 1. The inverse transform formula (1) is expressed as a coarse approximation furnished by scaling functions $\varphi_{0,k}$ on the bottom level mesh, and sets of wavelet functions $\psi_{j,k}$, representing the hierarchy of finer scale meshes, indexed by j

$$y = \sum_k \lambda_{0,k}\varphi_{J,k} + \sum_{j=0}^{N}\sum_k \gamma_{j,k}\psi_{j,k} \qquad (1)$$

where k is the location index, and y is the grid data. Wavelet coefficients γ_{jk} encode the difference between fine and coarse mesh representations of the underlying data, and are calculated by recursive filtering, with each step involving a "fine" (child nodes) and "coarse" (parent nodes) mesh [6].

Scale j	0	1	2	3	4	5	6
# Wavelets ψ_{jk}	3	9	30	108	408	1584	6240
Distance (km)	7000	3500	1750	880	440	220	110

Table 1: Wavelet basis details, pertaining to the inverse transform formula (1), on the quasi-uniform geodesic grid of Figure 1, where nominal refers to distance along a side of the original spherical equilateral triangle.

After filtering the entire ensemble according to (1), and associated verification at each analysis time, error and spread calculations are performed on each of the filtered components to yield a set of curves, each representing a scale from Table 1. Underlying these calculations are the wavelet coefficients γ_{jk}, of the ensemble mean error, which also deserve attention in their own right, for their local feature detection ability.

Tropical Cyclone Yasi

Tropical cyclone YASI [9] crossed the Queensland coast during the early hours of February 3, 2011. Most of its lifespan was captured by the ensemble forecast started at 18UTC on January 30, 2011, which culminates a few hours after landfall at T+72. At T+48, Figure 1 displays the ensemble mean MSLP error, together with a cyclone track estimate for the verifying analysis. A distinct positive error patch occurs over the cyclone, resulting from overprediction of the analysed central pressure, which is itself also an overprediction.

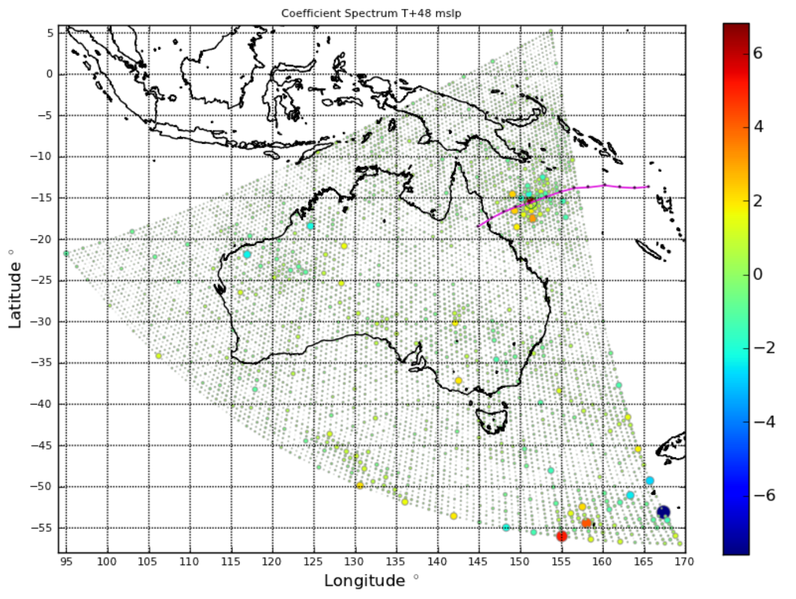

Figure 2: Wavelet domain view, or coefficient spectrum, for the mean MSLP error field in Figure 1, displaying all coefficients γ_{jk} from all levels.

In the wavelet domain, the mean MSLP error field of Figure 1 transforms to the coefficient spectrum of Figure 2, which simultaneously displays all coefficients γ_{jk} from all levels at their respective grid locations. The spectrum comprises a typical "sea" of small coefficients and a few local clusters of relatively large coefficients, representing signatures of particular features in the original domain of Figure 1. For the cyclone, a closer view appears in Figure 3.

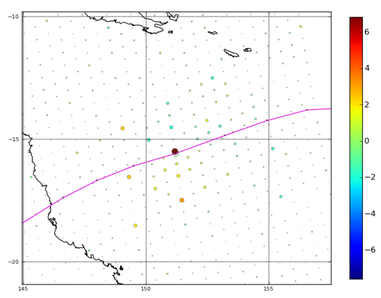

Figure 3: Zooming on error coefficient spectrum, in the cyclone track vicinity.

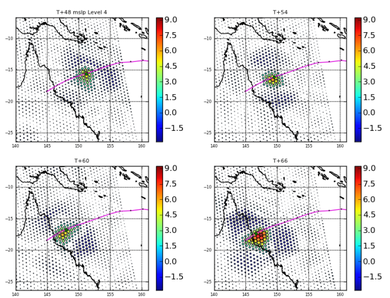

Figure 4: Level 4 mean error component time evolution, from T+48 to T+66.

Zooming on the cyclone vicinity in the coefficient spectrum of Figure 2 produces Figure 3, which shows a strong coefficient very close to the estimated analysis track. This "spectral peak", located within a grid spacing of the analysis track position estimate, actually belongs to level 4 ($\sim$ 450 km), indicating a key scale of interest. Reconstruction of this error component according to (1) at T+48, and subsequent times, produces the sequence shown in Figure 4, indicating a persistent "mexican hat" type structure, with highest strength at T+66, just before landfall.

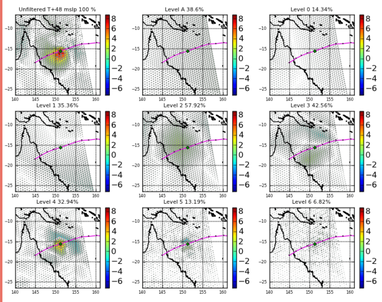

Figure 5: Ensemble mean MSLP error components at T+48.

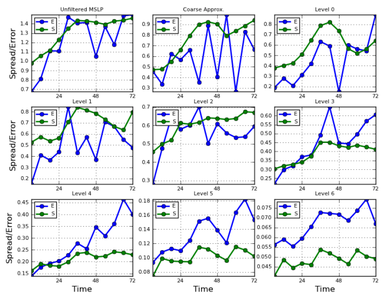

Figure 6: Multiscale error-spread curves for the TC YASI MSLP forecast.

Reconstructing all level components at T+48 gives the set of images in Figure 5, each of which is verified against its filtered analysis counterpart, along with the unfiltered version, at all forecast times up to T+72. The final domain averaged products are given in Figure 6, which is a set of multiscale error-spread curves, displaying fine scale underspreading for the forecast duration,(levels 5,6).

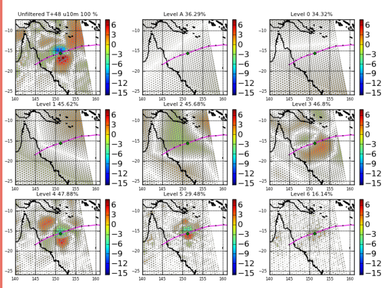

Figure 7: Ensemble mean 10m zonal wind error components at T+48.

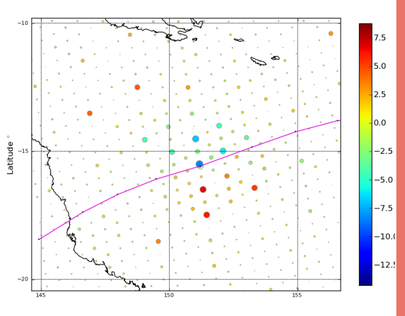

Figure 8: 10 metre zonal wind mean error wavelet coefficients, at T+48.

For the 10 metre zonal wind forecast, filtered error components at T+48 are shown in Figure 7. Negative and positive error lobes above and below the track in the unfiltered result, due to weaker mean wind components, are repeated on levels 4 and 5, and also reflected in the wavelet coefficients of Figure 8, again showing spectral peaks. Error-spread curves also exhibit fine scale underspreading for the forecast duration, as for MSLP in Figure 6.

Tropical Cyclones Carlos and Dianne

Two weeks after TC YASI, TC DIANNE and TC CARLOS were simultaneously active, DIANNE off the West Australian coast, and CARLOS in the Darwin area, both captured by an ensemble forecast started at 06UTC on February 16 2011. At T+48, the mean MSLP error field is shown in Figure 9, with associated wavelet coefficient spectrum in Figure 10. Distinct coefficient clusters appear over each cyclone, with the maximum absolute coefficient $|\gamma_{jk}|$ occurring on level 3 ($\sim$ 900 km), about 1 grid spacing from the DIANNE analysis track estimate.

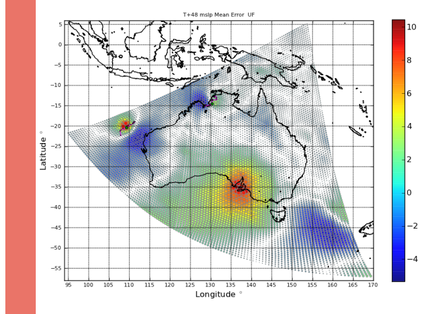

Figure 9: Mean MSLP error at T+48, cyclones DIANNE and CARLOS.

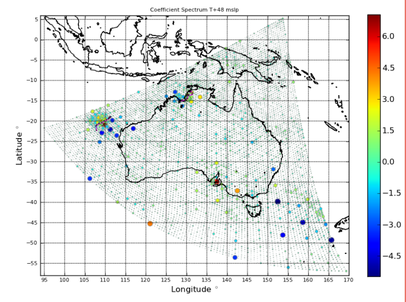

Figure 10: Wavelet coefficient spectrum for mean MSLP error at T+48.

The spectral peak on level 3 in the coefficient spectrum of Figure 10 invites examination of the corresponding reconstructed component, shown in Figure 11, which indicates complete domination of the larger cyclone DIANNE, and an unrelated strong error feature over the city of Adelaide, roughly 4000km away. On the next finer scale, level 4($\sim$ 450 km), cyclone CARLOS shows its distinct error features in the accompanying Figure 12.

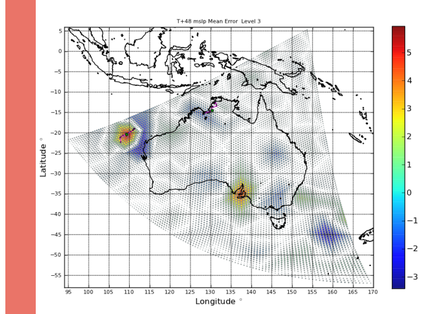

Figure 11: Level 3 mean MSLP error component at T+48.

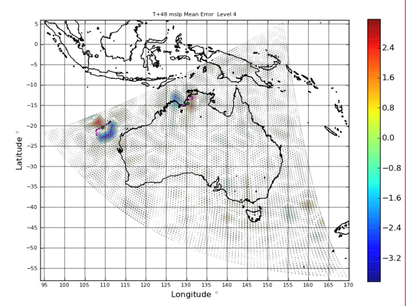

Figure 12: Level 4 mean MSLP error component at T+48.

For 10m zonal wind at T+48, the maximum absolute coefficient $|\gamma_{jk}|$ in the spectrum of Figure 13 occurs on level 3, at the same location and scale as that recorded for MSLP in Figure 10. Reconstruction of this error component produces the result in Figure 14, showing a strong contribution over TC DIANNE, which dwarfs that from the smaller TC CARLOS, as in the MSLP case of Figure 11.

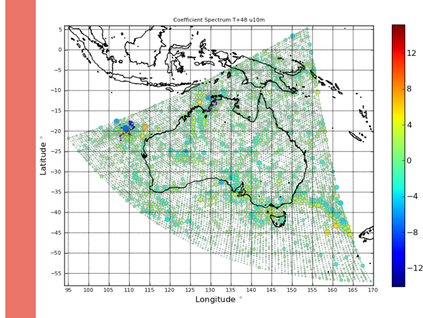

Figure 13: 10 metre zonal wind coefficient spectrum at T+48.

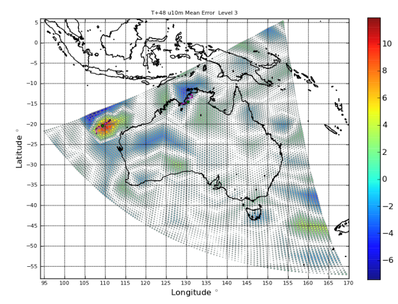

Figure 14: Level 3 mean U10M error component at T+48.

Repeating the multiscale error-spread curves for the DIANNE/CARLOS MSLP and 10 metre wind forecasts again displays fine scale underspreading for the entire duration.

Conclusions and Future Work

- Wavelet coefficient spectra for MSLP and 10m zonal wind ensemble mean error fields have produced spectral peaks close to the estimated cyclone analysis track.
- Fine scale underspreading was observed across the forecast duration for MSLP and 10 metre winds, in each case.
- More cyclones need to be examined in the multiscale framework, possibly with different wavelet bases.

References

[1] N. Bowler, A. Arribas et al., The MOGREPS short–range ensemble prediction system, *Q.J.R. Meteorol. Soc.* 134 p703–722 (2008).

[2] M. Carfora, Interpolation on spherical geodesic grids: A comparative study, *J. Comp. Appl. Math.* 210 p99–105 (2007).

[3] T. Jung and M. Leutbecher, Scale–dependent verification of ensemble forecasts, *Q.J.R. Meteorol. Soc.* 134 p973–984 (2008).

[4] D. Majewski et al., The Operational Global Icosahedral–Hexagonal Gridpoint Model GME: Description and High-Resolution Tests, *Mon. Wea. Rev.* 130 p319–338 (2002).

[5] K. Puri et al., 2010. Preliminary results from Numerical Weather Prediction implementation of ACCESS, *CAWCR Research Letters*, 5, p15–22 (2010).

[6] P. Schroder and W. Sweldens, Spherical Wavelets: Efficiently Representing Functions on the Sphere, (1995). http://www.multires.caltech.edu/pubs/sphwave.pdf

[7] D. Smith, M. Naughton and A. Sulaiman, Multiscale verification calculations for regional ensemble forecasts, *ANZIAM J.* 52 pC882–C898 (2011)

[8] http://www.gnu.org/software/octave/

[9] http://www.bom.gov.au/cyclone/history/yasi-mslp.shtml